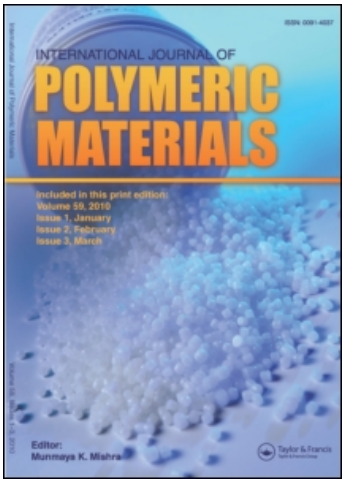

International Journal of Polymeric Materials
Publication details, including instructions for authors and subscription information:
http://www.informaworld.com/smpp/title~content=t713647664

Dynamics of an Explosion Blast-proof Aircraft Luggage Container. Part II—Theoretical Failure Analysis and Experimental Verification

H. B. Chin[a]; Y. D. Kwon[a]; H. L. Li[a]; D. C. Prevorsek[a]
[a] Corporate Technology Center, Allied Signal Inc., Morristown, N.J.

To cite this Article Chin, H. B. , Kwon, Y. D. , Li, H. L. and Prevorsek, D. C.(1994) 'Dynamics of an Explosion Blast-proof Aircraft Luggage Container. Part II—Theoretical Failure Analysis and Experimental Verification', International Journal of Polymeric Materials, 26: 1, 103 — 115
To link to this Article: DOI: 10.1080/00914039408029354
URL: http://dx.doi.org/10.1080/00914039408029354

Intern. J. Polymeric Mater., 1994, Vol. 26, pp. 103–115
Reprints available directly from the publisher
Photocopying permitted by license only

Printed in Malaysia

Dynamics of an Explosion Blast-proof Aircraft Luggage Container. Part II—Theoretical Failure Analysis and Experimental Verification

H. B. CHIN, Y. D. KWON, H. L. LI and D. C. PREVORSEK

Corporate Technology Center, AlliedSignal Inc., P.O. Box 1021, Morristown, N.J. 07962-1021

(Received February 10, 1994)

A theoretical analysis of the blast of an explosive and the effect of the blast on the walls of surrounding (neighboring) structure has been made using the finite element analysis technique. The finite element analysis computer code used in this analysis is EPIC-2 interfaced with the subroutines developed for the composite material behavior. EPIC-2 allows one to predict the explosion shock wave propagation and pressure field generated during the explosion. The effect of the shock wave on the neighboring structure during the explosion was analyzed. The stress levels within the neighboring structure were evaluated and the failure of the structure was predicted using appropriate failure criteria. The analysis results were then verified using the experimental data. This analysis procedure provides realistic results which are in good agreement with the experimental results. Experimental work was carried to assess the relative merits of Spectra vs. aramid in these applications.

KEY WORDS Polyethylene, ultra-strong fibers, spectra, explosion blast, failure analysis

1.0 INTRODUCTION

It has been recognized that Spectra fibers have outstanding impact resistance, high energy absorption and damage tolerance. Because of these superior characteristics of Spectra filbers, Spectra composites are most suitable for the applications concerned with protecting equipment or people against explosions or high speed ballistic projectiles. Among such applications, Spectra composites were identified as the best potential material for explosion proof luggage container for commercial aircraft.

Some experimental studies have been made on the behavior of Spectra composites against explosion, and explosion-proof luggage container development using Spectra composites is in progress by commercial companies, notably Jaycor, supported by FAA. In designing such containers, it is highly desirable to analyze the explosion phenomena to predict the performance of the Spectra composite used. In this paper, a rigorous analysis of the response of the Spectra composite during an explosion has been carried out using the finite element analysis technique.

The key factors responsible for the high impact energy absorption characteristics, namely strain rate dependent Spectra fiber properties, have been fully accounted for in the analysis and comparative studies also have been made with other ballistic materials such as metals, etc. The failure criteria of the materials analyzed have been established and verified by experimental data.

2.0 ANALYSIS METHOD

The analysis procedure used in this paper is first to predict the flow field and pressure field generated and shock wave propagation during the explosion. When the shock wave front reaches the neighboring structure, the response of the neighboring structure against the shock wave is predicted by solving the governing equations of momentum conservation. The stress levels and deformation of the structure are predicted and the failure of the structure is also predicted using failure criteria such as maximum strength, maximum strain criteria or erosion criteria. Thus the analysis simulate the phenomenon of an explosion and the failure or survival of the neighboring structures.

2.1 Analysis Procedure

The finite element analysis technique used to simulate the effects of an explosion on neighboring structures involves the following steps:

1. The geometry of the problem is discretized with an axisymmetric triangular element.
2. The distributed mass in the elements is lumped at the nodes.
3. The displacements and velocities at each node in the elements are determined.
4. The strains and strain rates in the elements are determined from the nodal displacements and velocities.
5. The stresses in the elements are determined using the constitutive relation of the material, and the equivalent forces at the nodes are determined from the stresses.
6. The equations of motion are applied to determine nodal accelerations and the new nodal velocities and displacements for the next time interval are determined by integration over the time increment.
7. The steps 5 through 7 are repeated until the time of interest has elapsed.

The analysis scheme is essentially to solve the equations of motion governing the explosion phenomena due to an explosive source. The governing equations of motion are given in tensorial form as

$$\sigma_{ij,j} = \rho \ddot{u}_i \tag{1}$$

where σ_{ij} are the stress components, ρ the density and $\ddot{u}_i$ is the acceleration vector. The stress components are decomposed into a hydrostatic pressure P and deviatoric stress components τ_{ij} as

$$\sigma_{ij} = -P\delta_{ij} + \tau_{ij} \tag{2}$$

where δ_{ij} is the Kronecker delta and $-P$ is defined as the mean of normal stresses, i.e.,

$$-P = \tfrac{1}{3}(\sigma_{11} + \sigma_{22} + \sigma_{33}) \tag{3}$$

The equation of continuity (conservation of mass) can be written as

$$\frac{d\rho}{dt} + \rho v_{i,i} = 0 \tag{4}$$

where ρ is density, v_i is velocity and $v_{i,i}$ is divergence of velocity. Alternatively, the conservation of mass can be expressed as

$$\dot{\varepsilon}_{ii} = \frac{\dot{V}}{V} \tag{5}$$

where $\dot{\varepsilon}_{ii}$ are the normal strain rates and V is the volume. The upper dot denotes the time derivative and the summation convention over repeated indices is implied. The strain components are given by

$$\varepsilon_{ij} = \tfrac{1}{2}(u_{i,j} + u_{j,i}) \tag{6}$$

The above governing equations are solved for both the explosive and the neighboring structure.

2.2 Formulation of Finite Element Analysis

Considering the axisymmetric nature of the problem, a two-dimensional axisymmetric triangular element was used in cylindrical coordinates. Then the field variables, e.g., radial displacement, within the element can be described by assuming that they vary linearly over each element,

$$u_r = \alpha_1 + \alpha_2 r + \alpha_3 z \tag{7}$$

where α_1, α_2 and α_3 can be expressed in terms of element coordinates and nodal values, yielding

$$u_r = \frac{1}{2A}[(a_i + b_i r + c_i z)u_i + (a_j + b_j r + c_j z)u_j + (a_k + b_k r + c_k z)u_k] \tag{8}$$

where A is the area of the element and

$$a_i = r_j z_k - r_k z_j, \quad b_i = z_j - z_k, \quad c_i = r_k - r_j \tag{9}$$

The other coefficients, a_j, b_j, c_j, etc., are obtained through a cyclic permutation of the subscripts i, j, k. The other displacements u_z and u_θ take the identical form except that the nodal values are replaced by axial and tangential values.

From the displacements, the strain in the elements can be obtained using Equation 6. The velocities and strain rates in the elements can be obtained in a similar manner to that used to determine displacements and strains. Note that since the displacements and velocities in the elements vary linearly, the strain and strain rates are constant in each element. The stresses in the elements are determined by Equation 2 depending on material behavior (constitutive equations). Having determined the stresses in the elements, the concentrated forces acting on the concentrated mass at the nodes are determined by following equations:

$$F_{ri} = -\pi\bar{r}[(z_j - z_k)\sigma_r + (r_k - r_j)\tau_{rz}] - \tfrac{2}{3}\pi A\sigma_\theta \tag{10}$$

$$F_{zi} = -\pi\bar{r}[(r_k - r_j)\sigma_z + (z_j - z_k)\tau_{rz}] \tag{11}$$

where r and z are the nodal coordinates and the net force at node i is the sum of the forces from individual element at that node.

The distributed mass in the elements is lumped at each node as

$$M_i = \tfrac{1}{3}V_0\rho_0 = \tfrac{2}{3}\pi\bar{r}_0 A_0\rho_0 \quad (i = 1, 2, 3) \tag{12}$$

where V_0, A_0 and ρ_0 are the initial volume, area and density of the element and $\bar{r}_0$ is the average of the initial radial coordinates of the element.

Now the equation of motion (Equation 1) is applied to each node using the lumped mass and concentrated forces and integrated to obtain the velocities and displacements for the next time step, assuming that the acceleration at each time step is constant. Thus the radial acceleration at node i at time t can be expressed as

$$\ddot{u}_r^t = \frac{\Sigma F_{ri}}{\Sigma M_i} \tag{13}$$

and the radial velocity and displacement at time $t + \Delta t$ are

$$\dot{u}_r^{t+\Delta t} = \dot{u}_r^t + \ddot{u}_r^t\,\Delta t \tag{14}$$

$$u_r^{t+\Delta t} = u_r^t + \dot{u}_r^t\,\Delta t + \tfrac{1}{2}\ddot{u}_r^t\,(\Delta t)^2 \tag{15}$$

The other components of velocity and displacements can be obtained in a similar manner and the entire process is repeated until the impact process is completed. The hydraulic pressure is determined from the equation of state known as Mie-Grüneisen equation:

$$P = (K_1\mu + K_2\mu^2 + K_3\mu^3)\left(1 - \frac{\Gamma\mu}{2}\right) + \Gamma\rho_0 I \tag{16}$$

where

$$\mu = \frac{\rho}{\rho_0} - 1 \tag{17}$$

K_1, K_2 and K_3 are material dependent constants and Γ is the Grüneisen coefficient. The specific internal energy, I, is obtained from the work done on the element. Detailed discussion on the finite element analysis technique can be found in the text books and literature.[1,2] Actual computation was performed using the computer code EPIC-2 which was interfaced with the subroutines developed to handle Spectra composite material and to accommodate our needs.

2.3 Spectra Composite Material Model

Spectra composite was assumed to be an orthotropic material as will be described below. The stress-strain relation of Spectra composites is now expressed as

$$\tau_i = C_{ij}\varepsilon_j \quad (i, j = 1, 2, \ldots, 6) \tag{18}$$

where C_{ij} are the elastic constants, and τ_i and ε_j are stresses and strains in a contracted notation of τ_{ij} and ε_{ij}, respectively. Since Spectra composites are orthotropic, there are nine independent elastic constants. These can be expressed in terms of conventional engineering constants and Poisson's ratios.

Experimentally, it has been observed that moduli of Spectra fiber are strain rate dependent as shown in Figure 1. Thus the moduli of the Spectra composites are also strain rate dependent. The properties of Spectra composites are then predicted from the properties of its constituents using the micromechanics and lamination theory. Since composite materials are heterogeneous from a microscopic point of view, it is assumed that the effective properties can be defined by using an averaging process over a characteristic volume element which is small enough to serve as the microstructure of the composite, yet large enough to represent overall behavior of the composite. The effective engineering constants (moduli) of unidirectional Spectra prepreg is first predicted from the moduli of the Spectra fiber and the matrix,

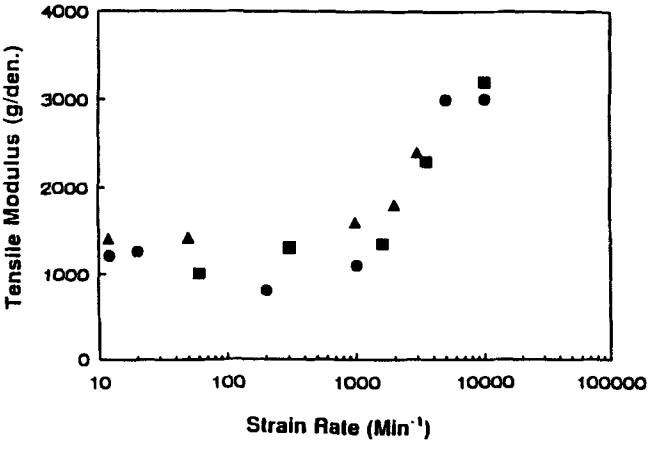

FIGURE 1 Strain dependent Spectra fiber modulus.

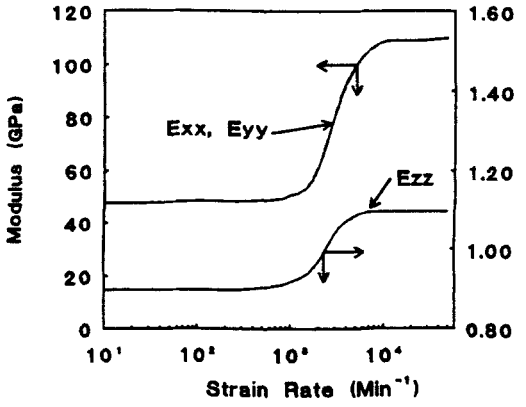

FIGURE 2 Strain dependent effective engineering moduli of Spectra composite (0/90 Spectra composite).

using the micromechanical model[3] and lamination theory.[4,5] Then, the effective engineering moduli of Spectra composite are predicted as:

$$E_{ij} = E_{oij} \text{ when } \dot{\varepsilon}_1 \leq \dot{\varepsilon}_0 \tag{19}$$

$$E_{ij} = C_{oij} + K_{oij} \log(\dot{\varepsilon}_i) \text{ when } \dot{\varepsilon}_0 \leq \dot{\varepsilon}_i \leq \dot{\varepsilon}_m \tag{20}$$

$$E_{ij} = E_{mij} \text{ when } \dot{\varepsilon}_i \geq \dot{\varepsilon}_m \tag{21}$$

where ε_0 and ε_m are material dependent strain rates. The strain dependent effective moduli of the Spectra composite are shown in Figure 2. These strain dependent engineering constants are used to determine C_{ij} in Equation (18) to describe the behavior of Spectra composite materials. The detailed discussion on the Spectra composite properties are given in the previous report.[6]

2.4 Failure Criteria

Spectra composite failure may be predicted from the strength of the Spectra fiber and matrix used. Various strength models for composite materials have been proposed in the literature based on various criteria. Two failure criteria were used in this analysis, i.e., maximum strength and maximum strain. The Spectra composite will fail if the strain exceeds the maximum strain and will erode if the stress exceeds the maximum strength. The maximum strength and strain were predicted using the quadratic interaction model.[7,8] Using this model, the failure envelopes for strength and strain were constructed and the maximum strength and strain for the Spectra composite were determined from the failure envelopes. In the analysis, when the strain in an element exceeds the maximum strain, the element is considered totally failed. The element will fracture if its stress exceeds the maximum strength but will not totally fail and the degree of fracture will be determined by the maximum strength and the stress level in the element.

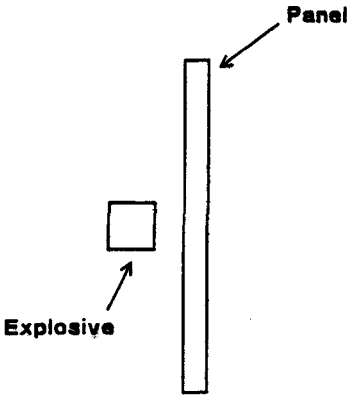

FIGURE 3 Experimental set-up of unconfined explosion.

3.0 EXPERIMENTAL

Explosion experiments were conducted with several explosives under confined and unconfined (open) conditions. In Figure 3, the schematic of unconfined explosion experiment set-up is shown. In the unconfined explosion experiment, a known amount of an explosive was placed against the test sample panel at a certain distance. The amount of the explosive and the distance from the test panel were varied. In the confined explosion experiment, a known amount of an explosive was placed at the center of the cubical box made of the test material (see Figure 4). The dimension of the box was 27″ × 27″ × 27″. The amount of the explosive used was varied.

4.0 RESULTS AND DISCUSSION

4.1 Explosion Simulation

The explosion of an explosive material was simulated and Figure 5 shows the propagation of the shock wave, where 1.0 oz of explosive was detonated against a 0.3 inch thick Spectra panel at a distance of 2.0 inches. It is seen that the shock wave front was reflected momentarily (at 20 microseconds) when it reached the panel. In Figure 6, the pressure field developed is shown for the case of the explosion of 1.0 oz of explosive against the Spectra panel at a distance of 1.0 inch. As time increases, the shock wave propagates and the pressure decreases with expanding shock wave front. The maximum pressure developed during the explosion is estimated to be of the order of 10^6 psi as can be seen from Figure 7. The shock wave propagation velocity is shown in Figure 8 which shows that the maximum shock wave propagation velocity is of the order of 10^5 inches per second. Figure 9 shows the equivalent stress (Von Mises stress) developed in the Spectra panel at 100 microsecond from the detonation of 1.0 oz explosive at a distance of 2.0 inches. The highest equivalent stress is of the order of 10^5 psi.

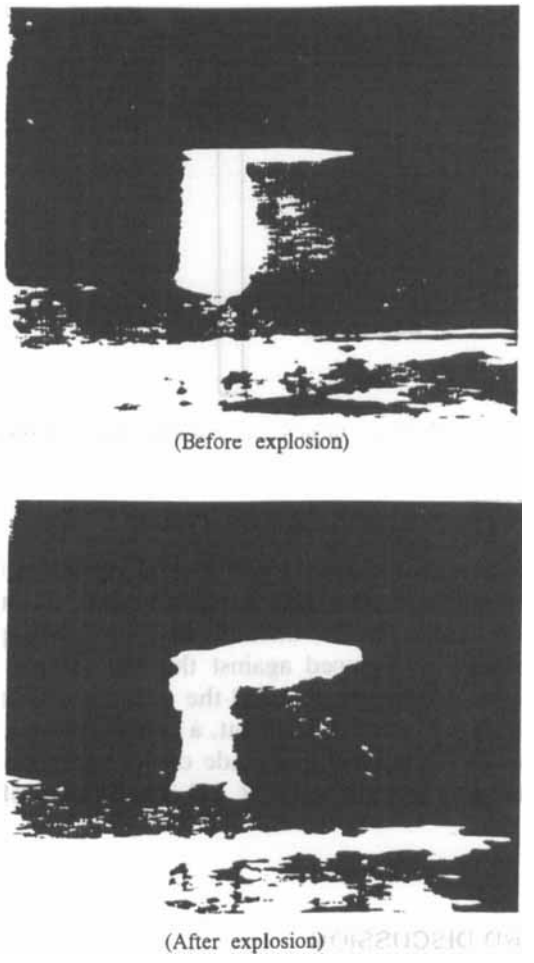

FIGURE 4 Experimental set-up of confined explosion.

4.2 Validation of Analysis

Theoretical simulation results of explosions of different amounts of explosive (Octol 78/22) against Spectra composite panel held at different distances from the explosive were compared with experimental results. The Spectra composite panel contain 70 wt% of Spectra fiber with 0/90 construction. The failure criteria were established from the comparison of experimental results conducted at the same conditions of simulation. The established failure criteria were then used in the simulations of the explosions against 0.3 inch thick Spectra panel held at different distances of from the explosive. The simulation results agreed very well with the experimental results. More simulations were performed with different target materials to further verify the simulation procedure. The comparison of the simulation results and the experimental results are shown in Table I. As can be seen from Table I, the simulation results are in very good agreement with the experimental results.

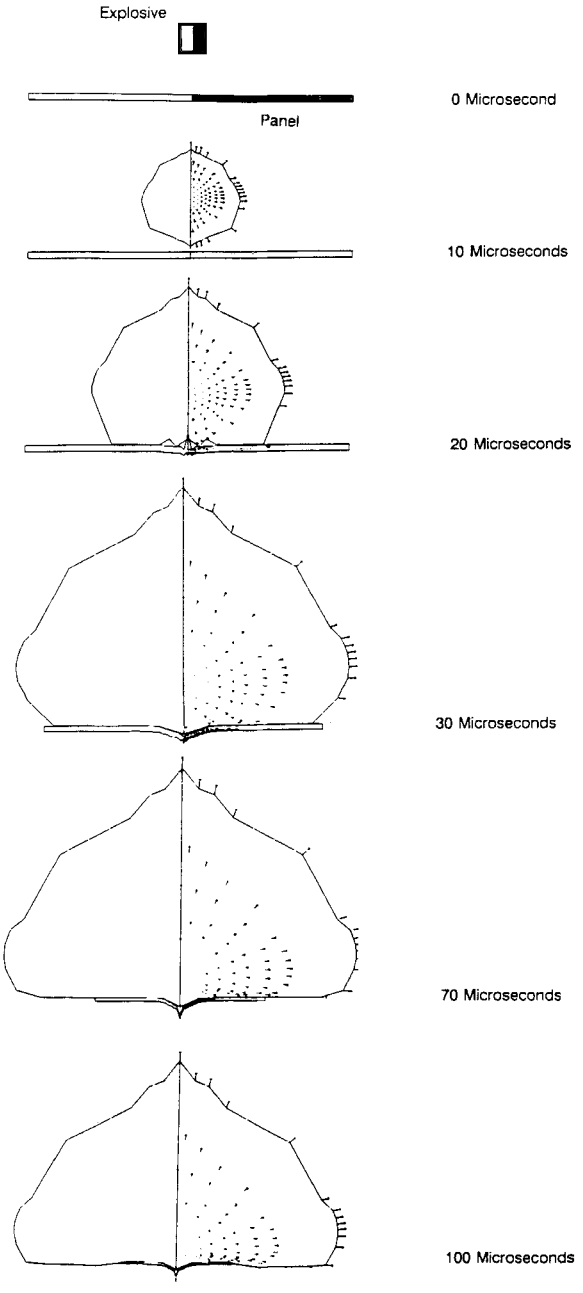

FIGURE 5 Shock wave propagation during explosion.

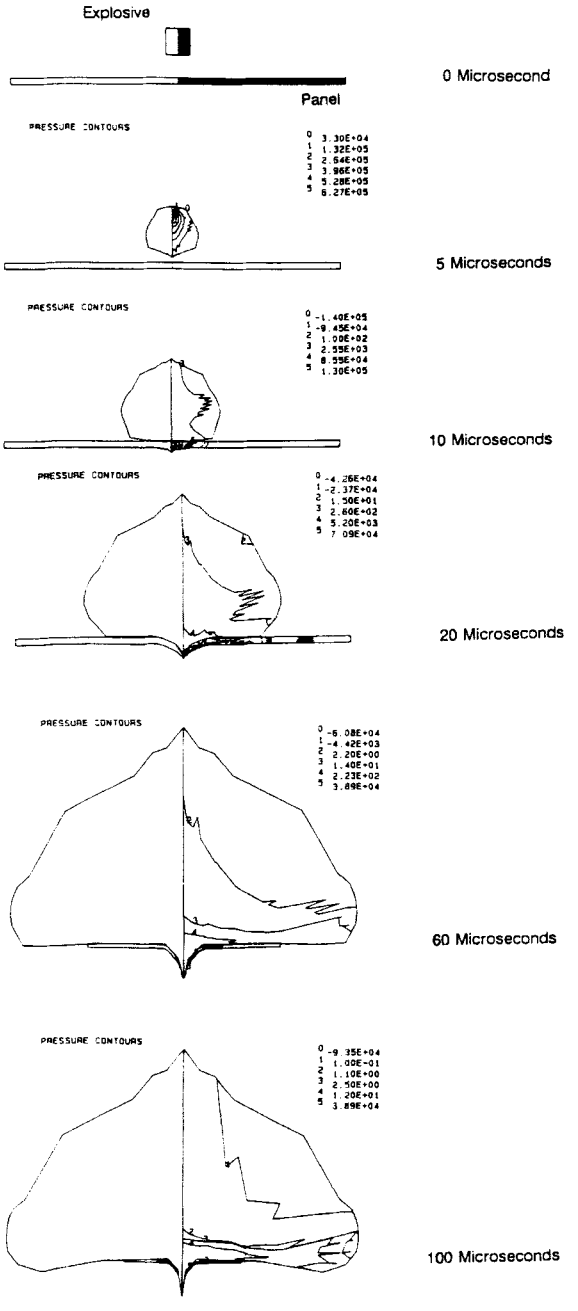

FIGURE 6 Pressure contours developed during explosion.

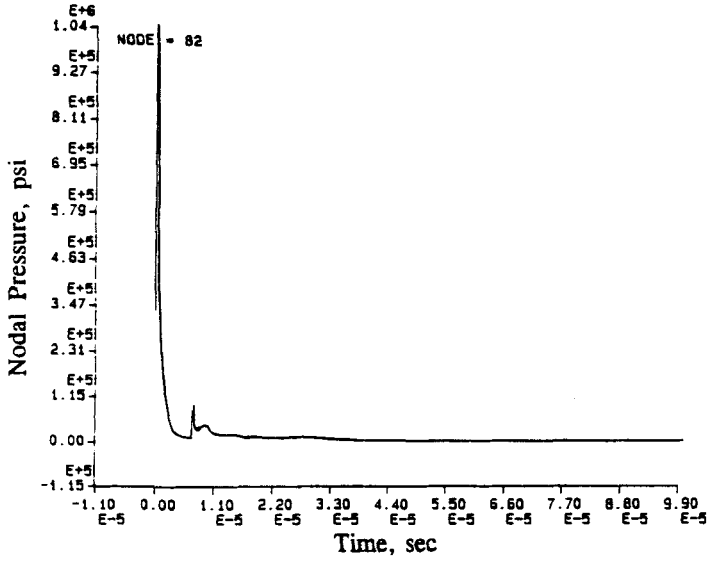

FIGURE 7 Pressure generated at the bottom of explosive during explosion.

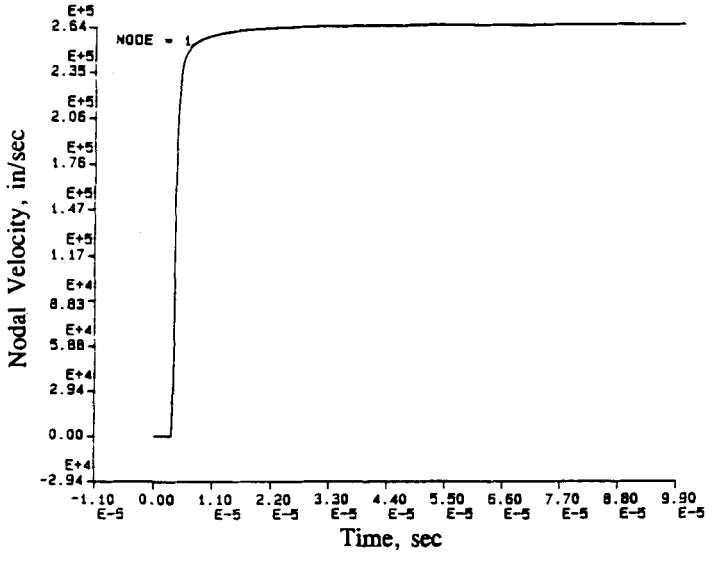

FIGURE 8 Shock wave front velocity (at the top of explosive).

4.3 Analysis of Confined Explosion

The main differences between confined and unconfined explosions are the effects of reflection of shock wave and pressure build-up due to confinement. The effects of the pressure build-up and the shock wave reflection depend on the volume of the confined space and the amount of explosive. As can be seen from Figures 5, 6 and 7, the pressure decreases rather rapidly as the shock wave front expands.

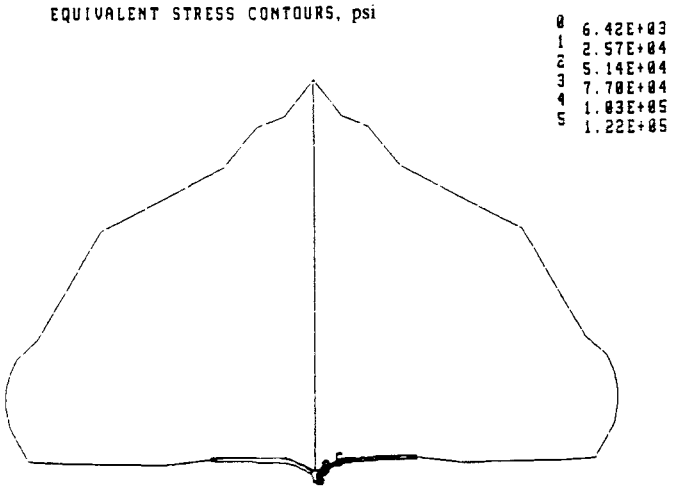

FIGURE 9 Equivalent stress (Von Mises stress) level at 100 microseconds.

TABLE I

Comparison of analysis results with experimental results (unconfined explosion)

Test Panel		Explosive	Distance	Analysis			Experiments		
Material	Thickness (in)	Size (oz)	(in)	Perforation	d (in)	D (in)	Perforation	d (in)	D (in)
Spectra	0.3	1.0	1.0	yes	2.6	6.0	yes	3.0	11.0
Spectra	0.3	1.0	2.0	no	1.0	8.0	no	1.5	11.5
Steel	0.077	1.0	1.0	yes	2.0	4.0	yes	4.5	9.0

Note: Spectra panel areal density: 7.26 (kg/m^2)
Steel panel areal density : 15.1 (kg/m^2)

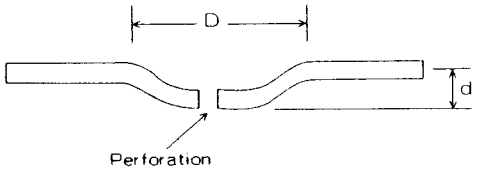

Thus the major damage to the neighboring structure will be caused by the shock wave if the structure is far from the explosive source.

For the case of the confined explosion experiment using a 27″ × 27″ × 27″ box, the effects of shock wave reflection and pressure build-up are insignificant compared to the effect of shock wave when the amount of explosive is less than 2.0 pounds. Thus the simulation of the confined explosion with the 27″ × 27″ × 27″ box was made the same way as that of unconfined explosion. The typical results are shown in Table II. As can be seen, the analysis results are realistic judging from the experimental results.

TABLE II

Comparison of analysis results with experimental results (confined explosion)

Test Box Material	Thickness (in)	Explosive Size (lbs)	Distance (in)	Analysis Failure	Experiments Failure
Spectra	0.17	0.5	13.5	no	no
Spectra	0.17	1.0	13.5	yes	yes
Aramid	0.15	0.5	13.5	yes	-

References

1. O. C. Zienkiewicz, "The Finite Element Method," 3rd Ed., McGraw-Hill, 1977.
2. G. R. Johnson, *Analysis of Elastic-Plastic Impact Involving Severe Distortions*, J. Applied Mechanics, ASME, 98, Series E, Sept. pp. 439–444, 1976.
3. J. C. Halpin and S. W. Tsai, Effects of Environmental Factors on Composite Materials, *Air Force Material Laboratory Technical Report, AFML-TR-67-423*, 1967.
4. J. C. Halpin, *Primer on Composite Materials: Analysis*, Technomic Publishing Co., Inc., Lancaster, Pa., 1984.
5. J. A. Whitney and R. L. McCullough, *Composites Design Guide*, Vol. 2, Section 2.1 Introduction to Anisotropic Elasticity, pp. 28–50 (1982).
6. D. C. Prevorsek, H. B. Chin, Y. D. Kwon, S. E. Sund and D. Hsieh, *Dynamics of an Explosion Blast Proof Aircraft Luggation Container, Part I*, Research Report No. 93-31, Project No. 010837.
7. S. W. Tsai and H. T. Hahn, *Introduction to Composite Materials*, Technomic Publishing Co., Inc., Lancaster, Pa., 1975.
8. S. W. Tsai and E. M. Wu, "A Theory of Strength for Anisotropic Materials," J. Composite Materials, Vol. 5, Jan. pp. 58–80, 1971.